Solution Methods for One-Dimensional Viscoelastic Problems

John M. Stubstad* and George J. Simitses†
Georgia Institute of Technology, Atlanta, Georgia

A recently developed differential methodology for solution of one-dimensional nonlinear viscoelastic problems is presented. Using the example of an eccentrically loaded cantilever beam-column, the results from the differential formulation are compared to results obtained from a previously published integral solution technique. It is shown that the results from these distinct methodologies exhibit a high degree of correlation with one another. A discussion of the various factors affecting the numerical accuracy and rate of convergence of these two procedures is also included. Finally, the influences of some "higher-order" effects, such as straining along the centroidal axis, are discussed.

Nomenclature

a	= load eccentricity
A	= area of cross section
E	= Young's modulus
$g(s,u)$	= Green's function for the spatial integrals
I	= moment of inertia
$J(t)$	= creep compliance
l	= length of cantilever
L_p	= Laplace transform operator
M, N	= moment and force resultant, respectively
P	= applied load
P_e	= Euler load
$\hat{s}, s$	= dimensional and nondimensional distance along the beam, respectively
t, τ	= time
u, w	= axial and transverse displacement, respectively
x, y	= spatial coordinates
γ_q	= Newton-Cotes quadrature weights
ϵ_0	= centroidal axis strain
κ	= curvature
ϕ	= angle of rotation

Introduction

A NUMBER of solution methods are available for viscoelastic problems in which the behavior of the material may be adequately characterized by a linear viscoelastic operator and where the deformation of the body is sufficiently small to allow the use of a linear kinematic formulation.[1,2] Commonly, integral transform methods, separation of variables, series expansions, and other techniques provide methodologies wherein exact closed-form solutions may be derived. When exact solutions cannot be obtained, approximate techniques, such as one proposed by Schapery,[3] provide an alternate approach.

The inclusion of nonlinear effects in the analysis significantly reduces the mathematical tractability of the problem. These nonlinear influences can be induced by geometric factors resulting from the magnitude of the deformation or from gross rotation of cross sections. Alternatively, nonlinearities in the material response may need to be included to provide an accurate model for material behavior.

Independent of whether the nonlinearities are produced by geometric or material effects, they invariably result in nonlinear governing equations. Thus, the solution methods mentioned here, applicable to linear problems, generally cannot be employed. Approximation methods,[4] however, have been developed and can be employed to analyze such problems.

One of these methods is to idealize the problem in a manner that inherently simplifies the governing relations. An example of this technique was the utilization of an ideal "I" cross-sectional geometry in early column creep-buckling studies.[5] With this approximation, the equilibrium equations were reduced to simpler forms, involving the "average" stresses in the ideal flanges, where closed-form solution was possible.

Another approach used extensively was to restrict considerations to only certain types of time-dependent material behavior.[6] In some cases, this involved retaining only secondary creep behavior in the material model. Alternatively, and especially when "power-law" type constitutive laws were used, the constants or exponents of the law were restricted to special values for which closed-form solution was possible.[7] In a few cases, this approximation, as well as the aforementioned geometric simplification technique, were employed simultaneously to enable solution. A survey of many of these techniques has been provided by Hoff.[8]

A more general technique for the solution of geometrically nonlinear viscoelastic problems was first presented by Rogers and Lee.[9] In this method, the solution was formulated as an integral equation that was nonlinear in both time and space. From this, numerical results were obtained using computational techniques. A recent paper by the authors[10] provided a method for bounding the solution of problems formulated in this manner.

Generally, both the exact and bounding technique can be employed for problems wherein the response of the material may be adequately characterized using a linear viscoelastic model, but where the resulting time-dependent deformation of the body warrants the use of a nonlinear kinematic formulation. Problems involving nonlinear viscoelastic material behavior, however, currently cannot be addressed with this method. Unfortunately, many materials, and especially the elevated temperature behavior of most metals, require a nonlinear constitutive characterization. Consequently, an alternate solution procedure for one-dimensional problems involving nonlinear kinematic and nonlinear material effects has been developed. This method, hereinafter referred to as the differential formulation, is based on the direct solution of the nonlinear differential equations of equilibrium.

Similar to the integral method, the differential formulation is predicated on the assumption of a quasistatic response. This, effectively, "decouples" the temporal and spatial dependence of the problem in a manner that allows the general solution to be treated as the sequential combination of solutions to a nonlinear "boundary value" problem and a nonlinear "initial value" problem. The first of these, the equations characterizing the time-dependent states of quasistatic equilibrium, are solved

Presented as Paper 87-0804 at the AIAA/ASME/ASCE/AHS 28th Structures, Structural Dynamics and Materials Conference, Monterey, CA, April 6–8, 1987; received May 27, 1987; revision received Aug. 27, 1987.

*Former Graduate Research Assistant, School of Engineering Science and Mechanics. Member AIAA.

†Professor of Aerospace Engineering. Associate Fellow AIAA.

through the use of a Newton-type method.[11] The "initial value" problem, resulting from the nonlinear constitutive law, governs the manner by which the body progresses from one state of quasistatic equilibrium to the succeeding one. Numerical solutions for this part of the problem are generated using a fourth-order Runge-Kutta method. This general method has recently been employed to examine the nonlinear thermoviscoelastic behavior of thin structural members.[12]

In addition to presenting the differential formulation technique, a comparison of results obtained using the integral and differential formulations is provided. The problem of an eccentrically loaded viscoelastic cantilever beam-column is employed as the vehicle through which the comparison is performed. Because of the inherent limitation of the integral technique, this comparison is restricted to the consideration of a linear viscoelastic material. The specific case considered is that of the three-parameter viscoelastic solid, which has been examined in a number of studies.[10,13,14] The results obtained from these two distinct methods of solution exhibit a surprisingly high degree of correlation with one another, thereby establishing a high level of confidence in the validity of the methods. Finally, the differential formulation is employed to examine the influences of some "higher-order" effects in the class of problems under consideration.

Integral Formulation

The Rogers and Lee formulation method,[9] hereafter referred to as the integral solution technique, is focused toward formulating the solution to the nonlinear viscoelastic problem in terms of an integral equation. The general method was evolved through analogy to the associated geometrically nonlinear elastic problem. Only a synopsis of the method is presented here since complete developments for the technique are available in the literature.[9,10]

In the integral formulation, the time dependence of the material behavior is expressed in the form of a Volterra-type integral operator. This operator acts upon a second integral expression, which characterizes the quasistatic equilibrium of the body. For application to beam-column-type problems, it is assumed that the beam-column is thin and composed of a linearly viscoelastic material. In addition, referenced line extensional strains are assumed to be negligibly small. Thus, the coordinate $\hat{s}$, denoting distance along the undeformed length, can be employed to specify position in both the initial and deformed configurations. For convenience, a nondimensional coordinate s is defined by dividing $\hat{s}$ by the length of the beam l. Figure 1 illustrates a typical geometry used with this method. For the sample problem, the eccentric load is assumed to be applied quasistatically, and its direction does not vary with time.

Assuming a linear distribution of the strains through the depth, bending, thus occurring within an Euler-Bernoulli context, results in a moment-curvature relationship of the form

$$\kappa(\hat{s},t) = \left(\frac{1}{I}\right)\int_{-\infty}^{t} J(t-\tau)\left[\frac{\partial M(\hat{s},\tau)}{\partial \tau}\right]\mathrm{d}\tau \tag{1}$$

where $\kappa(\hat{s},t)$ denotes the curvature and $M(\hat{s},\tau)$ the bending moment at location $\hat{s}$. I denotes the moment of inertia of the beam and $J(t)$ the creep compliance of the material. For the sample problem, the moment at position $\hat{s}$ would be given by

$$M(\hat{s},\tau) = P(\tau)[\delta(\tau) + a\cos\alpha(\tau) - y(\hat{s},\tau)] \tag{2}$$

where $P(\tau)$ denotes the load applied at eccentricity α. Since

$$\kappa(\hat{s},t) = \frac{\partial \phi(\hat{s},t)}{\partial \hat{s}} \tag{3}$$

then, for quiescent initial condition, the Laplace transformation of Eq. (1) yields

$$\frac{\partial \Phi(s,p)}{\partial s} = \frac{l}{I}pJ(p)L_p[M(s,t)] \tag{4}$$

where J(p) and $\Phi(s,p)$ denote the transforms of $J(t)$ and $\phi(s,t)$, respectively, and where p represents the Laplace variable. Note that the nondimensional coordinate s has also been employed in the preceding expression.

Assuming that the Laplace variable apears only algebraically, Eq. (4) has the form of a type of "ordinary" differential equation. Consequently, integrating with respect to s yields

$$\Phi(s,p) - \Phi(0,p) = \frac{l}{I}pJ(p)L_p\left[\int_0^s M(r,t)\,\mathrm{d}r\right] \tag{5}$$

Note that the order of integration and Laplace transformation has been interchanged. This is a direct result of the assumption of inextensionality; consequently, s and t represent independent variables.

Equation (5) reveals a very interesting aspect of this formulation. Namely, the underlying structure of the equation is completely determined by the manner in which the moment depends on the deformation. For example, even if the moment depends upon the spatial coordinate s, provided it is independent of the deformation, then the basic equation is, in principle, integrable to a closed-form solution. This solution is, in fact, the usual result obtained from a linear analysis.

Illustrating how the equation structure changes when the moment is related to the deflection is best demonstrated through analogy with the associated elastic problem. Note that the governing relation for the associated elastic problem can be obtained by replacing the creep compliance by the elastic compliance and eliminating the Laplace operator. This yields

$$\phi_e(s) - \phi_e(0) = \frac{l}{EI}\int_0^s M(r)\mathrm{d}r \tag{6}$$

Note that the governing equation for the associated elastic problem takes on the form of a linear Fredholm equation when the moment depends linearly upon the deflection. In contrast, a nonlinear Fredholm format is obtained for cases where the moment is nonlinearly dependent upon deformation. In a similar manner, the viscoelastic problem takes on a linear "quasi-Fredholm" form when the moment is linearly dependent upon the deformation. A nonlinear "quasi-Fredholm" format occurs when, as in the sample problem, the relationship between moment and deflection is nonlinear.

To complete the formulation for the sample problem, Eqs. (2) and (3) are substituted into Eq. (1). Following differentiation with respect to s, the kinematic relations

$$\begin{aligned}\frac{\partial x(\hat{s},t)}{\partial \hat{s}} &= \cos\phi(\hat{s},t)\\ \frac{\partial y(\hat{s},t)}{\partial \hat{s}} &= \sin\phi(\hat{s},t)\end{aligned} \tag{7}$$

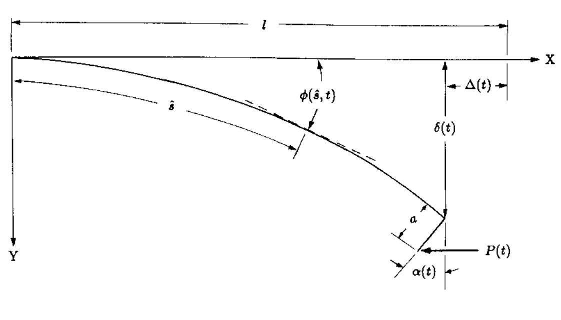

Fig. 1 Beam-column geometry for the integral method.

are employed to express all deformation-related quantities in terms of ϕ. For the sample problem, the boundary conditions are

$$\phi(0,t) = 0$$
$$M(l,t) = aP(t) \cos\phi(l,t) \tag{8}$$

where $\alpha(t) = \phi(l,t)$ for a "rigid" extension. Thus, using the methodology detailed in Ref. 9 and assuming quiescent initial conditions yields the solution

$$\phi(s,t) = \left(\frac{l^2}{I}\right)\left[J(0)P(t)\Theta(s,t) + \int_0^t J'(t-\tau)P(\tau)\Theta(s,\tau)\,\mathrm{d}\tau\right] \tag{9}$$

where

$$\Theta(s,t) = \left(\frac{sa}{l}\right)\cos\phi(1,t) + \int_0^1 g(s,r)\sin\phi(r,t)\,\mathrm{d}r \tag{10}$$

and

$$g(s,r) = r, \qquad 0 \le r \le s$$
$$= s, \qquad s \le r \le 1 \tag{11}$$

Note that the prime in Eq. (9) denotes differentiation with respect to the argument of the function.

Equation (9) represents a time convolution of a nonlinear spatial integral equation, Eq. (10). Numerical solutions are obtained using Picard's method of successive substitutions.[15] Newton-Coates formulas are used to approximate the spatial integral, and a fixed-step trapezoidal rule is employed for the time convolution. The general format of the algebraic expressions obtained in this manner is

$$\phi(s_i,t_n) = \frac{\pi^2}{4}\frac{P}{P_e}\Delta t\left[\left(1 + \frac{1}{2}J'(0)\right)\Theta(s_i,t_n) + \sum_{j=2}^{n-1} J'(t_n - t_j)\Theta(s_i,t_j) + \frac{1}{2}J'(t_n)\Theta(s_i,0^+)\right] \tag{12}$$

with

$$\Theta(s_i,t_j) = \frac{s_i a}{l}\cos\phi(1,t_j) + \Delta s\left[\sum_{k=1}^{i} \gamma_k r_k \sin\phi(r_k,t_j) + \sum_{k=i}^{p} \gamma_k s_i \sin\phi(r_k,t_j)\right] \tag{13}$$

Note that in Eq. (12), the number of terms in the summation increases linearly with each succeeding time step, whereas the number of terms in the summations represented by Eq. (13) is fixed. This increasing summation requirement in Eq. (12) has a significant impact on the relative speed of the integral formulation computations.

Differential Formulation

As previously noted, the differential formulation technique is based on the direct solution of the governing differential equations. Similar to the integral formulation, the differential formulation is also based on the assumption of quasistatic behavior. From this, the equations governing the successive states of quasistatic equilibrium may be expressed in terms of deformation functions and force and moment resultants. Consequently, these equations have the general format of a nonlinear boundary value problem. A Newton-type method, first suggested by Thurston,[11] is employed to derive solutions for this part of the problem.

On the other hand, the constitutive law, expressing the time dependence of the material response, governs the evolution of the force and moment resultants as the system progresses between successive states of quasistatic equilibrium. This represents a form of initial value problem with the values of the constitutive variables, such as accumulated viscoelastic strain, providing the initial conditions. For a nonlinear constitutive law, numerical procedures such as a Runge-Kutta or Euler method may be employed to predict the growth of these variables. Note that, for a "beam-theory" type formulation such as this, a spatial integration of the viscoelastic strain across the cross section is also required to enable evaluation of the force and moment resultants.

Similar to the integral formulation, the differential formulation for the sample problem is also based on the assumption that bending of the beam occurs in accordance with the Euler-Bernoulli hypotheses. Employing the functions $u(s,t)$ and $w(s,t)$ to denote, respectively, the axial and transverse deflection of the centroidal axis, then the extensional strain at the centroidal axis ϵ_0 is approximately given by

$$\epsilon_0 \approx \frac{\partial u}{\partial s} + \frac{1}{2}\left(\frac{\partial w}{\partial s}\right)^2 \tag{14}$$

Note that the term $\frac{1}{2}(\partial u/\partial s)^2$ has been neglected as small in comparison to $\partial u/\partial s$. If, in addition, both the strain at the centroidal axis and $\partial u/\partial s$ are small in comparison to 1, then it is simple to show that

$$\frac{\partial\phi}{\partial s} \approx \frac{\partial w}{\partial s}\frac{\partial^2 u}{\partial s^2} - \frac{\partial^2 w}{\partial s^2} \tag{15}$$

where ϕ denotes the angle of rotation of the cross section. Thus, the assumption of a linear variation of strain across the cross section yields

$$\epsilon_{11} = \epsilon_0 + \eta\frac{\partial\phi}{\partial s} \tag{16}$$

Employing the principal of virtual work followed by integration by parts and subsequent algebraic manipulation yields the equilibrium equations

$$N = -F\left\{1 + \frac{\partial\phi}{\partial s}[a\cos\phi(l) + w(s) - w(l)]\right\} \tag{17a}$$

$$M = F[a\cos\phi(l) + w(s) - w(l)] \tag{17b}$$

where N and M, the force and moment resultants, respectively, are defined as

$$N = \int_A \sigma_{11}\mathrm{d}A \tag{18a}$$

$$M = \int_A \eta\sigma_{11}\mathrm{d}A \tag{18b}$$

Based on an additive decomposition for the total strain, $\epsilon_t = \epsilon_e + \epsilon_c$, where ϵ_e and ϵ_c represent the elastic and creep strain components, respectively, yields, after substitution into Eqs. (17) and (18),

$$EA\epsilon_0 = -F\left\{1 + \frac{\partial\phi}{\partial s}[a\cos\phi(l) + w(s) - w(l)]\right\} + N_c \tag{19a}$$

$$EI\frac{\partial\phi}{\partial s} = F[a\cos\phi(l) + w(s) - w(l)] + M_c \tag{19b}$$

where the "pseudoresultants" N_c and M_c are defined by

$$N_c = \int_A E\epsilon_c\mathrm{d}A \tag{20a}$$

$$M_c = \int_A \eta E\epsilon_c\mathrm{d}A \tag{20b}$$

Numerical solution for Eqs. (19) are computed using a modified Newton-type method suggested by Thurston.[11] To illustrate this method, consider a nonlinear differential term of the form $du^m dw^n$ where du and dw are differentials of the functions u and w and m and n represent integer exponents. Assuming that close trial solutions $\tilde{w}$ and $\tilde{u}$ are available, which differ from the exact solution by the small quantities Δw and Δu so that $u = \tilde{u} + \Delta u$ and $w = \tilde{w} + \Delta w$, then

$$du^m dw^n = d\tilde{u}^m d\tilde{w}^n + m d\tilde{u}^{m-1} d\tilde{w}^n d(\Delta u) + n d\tilde{u}^m d\tilde{w}^{n-1} d(\Delta w) + f(\tilde{u},\tilde{w}) O[\Delta u, \Delta w] \tag{21}$$

where $f(\,)$ denotes a nonlinear function of $\tilde{u}$ and $\tilde{w}$ and $O[\,]$ indicates terms of order $\Delta u \Delta w$ and higher. If the trial solution is indeed close to the true solution, then the corrections Δu and Δw will be small. Consequently, the quadratic and higher-order terms in the corrections will be negligible in comparison to the linear terms and therefore may be neglected. Thus, the left-hand side of Eq. (21) may be closely approximated by the linearized form consisting of just the first three terms on the right-hand side.

With this procedure, the original nonlinear differential equation is approximated by a linearized form. Employing standard finite-difference formulas, the linearized form is then converted into a system of algebraic equations where the unknowns are the corrections to the trial solution at the nodes of the finite-difference mesh. These relations are solved for these corrections, the trial solution is adjusted, and the process repeated until convergence is obtained.

Application of this procedure to the geometry of the sample problem, e.g., yields the finite-difference expressions

$$\begin{aligned} & EI\frac{\partial \tilde{w}_i}{\partial s}\Delta u_{i-1} - 2EI\frac{\partial \tilde{w}_i}{\partial s}\Delta u_i + EI\frac{\partial \tilde{w}_i}{\partial s}\Delta u_{i+1} \\ & - EI\left(1 + 2\Delta s\frac{\partial^2 \tilde{u}_i}{\partial s^2}\right)\Delta w_{i-1} + (2EI - \Delta s^2 P)\Delta w_i \\ & - EI\left(1 - 2\Delta s\frac{\partial^2 \tilde{u}_i}{\partial s^2}\right)\Delta w_{i+1} + \Delta s^2 P \Delta w_n \\ & + 2\Delta s P a \tan\tilde{\phi}(\Delta w_{n-1} - w_{n+1}) \\ & = \Delta s^2\left[M_i^* + M_{c_i} - EI\frac{\partial \tilde{\phi}_i}{\partial s}\right] \end{aligned} \tag{22a}$$

and

$$\begin{aligned} & M_i^*\left(\frac{\partial \tilde{w}_i}{\partial s} - 2\Delta s EA\right)\Delta u_{i-1} - 2M_i^*\frac{\partial \tilde{w}_i}{\partial s}\Delta u_i \\ & - M_i^*\left(\frac{\partial \tilde{w}_i}{\partial s} + 2\Delta s EA\right)\Delta u_{i+1} \\ & - \left[2\Delta s EA\frac{\partial \tilde{w}_i}{\partial s} + M_i^*\left(2\Delta s\frac{\partial^2 \tilde{u}_i}{\partial s^2} + 1\right)\right. \\ & \left. + 2\Delta s P \tan\tilde{\phi}_i\right]\Delta w_{i-1} + \left(\frac{\partial \tilde{\phi}_i}{\partial s}\Delta s^2 P + 2M_i^*\right)\Delta w_i \\ & + \left[2\Delta s EA\frac{\partial \tilde{w}_i}{\partial s} + M_i^*\left(2\Delta s\frac{\partial^2 \tilde{u}_i}{\partial s^2} - 1\right)\right. \\ & \left. + 2\Delta s P \tan\tilde{\phi}_i\right]\Delta w_{i+1} - \frac{\partial \tilde{\phi}_i}{\partial s}\Delta s^2 P \Delta w_n \\ & - 2\frac{\partial \tilde{\phi}_i}{\partial s}\Delta s P a \tan\tilde{\phi}_n(\Delta w_{n-1} - \Delta w_{n+1}) \\ & = \Delta s^2\left[-P\cos\tilde{\phi}_i + N_{c_i} - E\tilde{\epsilon}_0 - M_i^*\frac{\partial \tilde{\phi}_i}{\partial s}\right] \end{aligned} \tag{22b}$$

where

$$M_i^* = P(a\cos\tilde{\phi}_n + \tilde{w}_i - \tilde{w}_n) \tag{23}$$

In these equations, the subscript i is used to represent interior nodes, and the subscript n is employed to indicate the node at the loaded end of the beam-column. Values obtained from the trial solution have been denoted by the placement of a tilde over the applicable term.

Numerical solution of Eqs. (22) requires evaluation of the "pseudoresultants" N_c and M_c at each interior point of the finite-difference mesh. This is accomplished by evaluating the accumulated creep strain at a select number of points across the cross section at each of the axial nodes. A three-point Newton-Cotes quadrature formula is then employed repetitively to approximate the area integrals. For the sample calculations reported herein, evaluation of the accumulated creep strain at each of these points is accomplished through the use of a fourth-order Runge-Kutta integration routine to integrate the constitutive law.

Example Problem

The specific example considered is that of a 30.5 cm (12 in.) long beam-column. For simplicity, a square cross section of dimension 12.7 mm (0.5 in.) has been assumed. It is also assumed that the beam-column is fabricated from a material that can be modeled as a three-parameter viscoelastic solid. The creep compliance for this model, illustrated in Fig. 2, is given by

$$J(t)/J(0) = 1 + [E_2/E_1]e^{-t/\tau_0} \tag{24}$$

where $\tau_0 = v_1/E_1$. For the sample computations, the numerical values for the parameters have been selected so that $\tau_0 = 1$. Thus, integer values for time t are equal to multiples of the time constant of the material. The elastic modulus of the material, E_2, is assumed to be 196 GPa (28.5×10^6 psi), the room temperature modulus of Hastelloy X.

A five-point grid in the transverse direction is used in computing the "pseudoresultants" in the differential formulation. The points are equidistantly spaced, with the first and last located at the extreme fibers and the central point positioned on the centroidal axis.

Since the governing equations of both the differential and integral formulations are only satisfied at a discrete number of points over the length of the beam-column, the first question addressed is the sensitivity of the results to the number of points used in the approximation. Table 1, for example, compares initial elastic deflections determined using the differential formulation as the number of approximating points is doubled from 10 to 20 and then doubled again to 40. Table 2 provides a similar comparison for the integral formulation.

It can be seen that there is very little change in the computed transverse deflection as the number of approximating points is increased. In both cases, the initial elastic solution for the 10-element model is within 1.0% of the 40-element model results. Additionally, the relative magnitude of the errors between the 10- and 40- as well as the 20- and 40-element models of the differential formulation are very similar to those exhibited by the equivalent comparison of integral solution models. These specific results, of course, apply for an eccentricity ratio of 0.05 and an applied load of $P/P_e = 0.75$, where the Euler load P_e is based on a perfect geometry and use of the instantaneous compliance of the material $J(0)$. However, they, like other results reported herein, illustrate the general trends observed at other load levels and load eccentricities.

Thus, both formulations exhibit a similar low sensitivity to the number of elements used in the analysis. Concurrently, the results also indicate that a 10-element model can be used with either method without generating significant errors in the analysis. It should be noted that all of the differential formulation results presented in the first table are based on the use of an exact expression for evaluating the angle of rotation. The influence of employing an approximate formula for calculating the angle of rotation is discussed in a later section. Also note that at this load and eccentricity, the initial end rotation of the beam-column exceeds 17 deg. Of course, smaller rotations are exhibited at the lower loads and lower eccentricities. Higher loads and larger eccentricities, conversely, produce greater rotations.

A direct comparison between the results generated by the two formulations is provided in Tables 3 and 4. Again, the comparison is based on the 0.05 eccentricity ratio, which produces reasonably large angles of rotation. Angles of rotation of the cross section, determined from the integral technique, are included in the tabulated data.

It should be noted that the differential solution results presented in Table 3 are based on the use of an exact expression for evaluation of $\sin\phi$. Differential solution results obtained using an approximate expression for $\sin\phi$ are provided in Table 4. The common approximation $\phi \approx \sin^{-1}(-\partial w/\partial s)$ is employed to calculate the angle of rotation for this second set of results. Except for this particular difference, these two differential formulations are otherwise completely identical.

These results indicate that little difference exists between the initial deformation predicted using the integral formulation and that predicted by either differential solution. The differences between the integral and differential methods are typically an order of magnitude lower than the differences observed for either technique when the number of elements was quadrupled. A potentially high-order effect may be indicated by the relative increase in differences at the highest loading examined. However, despite this increase, the magnitude of the differences is still so small as to be completely inconsequential with regard to engineering computations.

The data also indicate that no significant differences in the differential formulation (predicted transverse deflections) occur as a result of using an approximate formula for evaluation of $\sin\phi$. Even for an end rotation angle of 17 deg, the exact and approximate results differ only in the third or fourth decimal place. It should be noted that this high level of correlation continues to exist for even greater angles of rotation.

The probable reason for this high correlation is that, under compressive loading, the derivative of the axial displacement is negative. With reference to Eq. (14), this implies that the centroidal axis strain is numerically equal to the difference between the two components since the squared term (slope of the transverse deflection) is always positive. Thus, the magnitude of the centroidal axis strain must be less than the magnitude of either of its components. Because the difference between the exact and approximate expressions for $\sin\phi$ is related to the $\sqrt{1+2\epsilon_0}$ in the denominator of the exact expression, reducing the magnitude of the centroidal strain must inherently improve the accuracy of an approximation where this term is neglected.

This is best illustrated by the data of Table 5. Here, the integral solution is compared to an approximate differential solution in which the effect of the centroidal axis strain terms are suppressed. This suppression is accomplished by eliminating all the $(\partial w/\partial s)^2$ terms from the governing equations. In addition, the EA modulus-area product is artificially increased through multiplication by a factor of 1000. This second change reduces the magnitude of the axial deflections u by approximately the same factor. The overall intent of this effort was to create a differential model that would simulate the axial "inex-

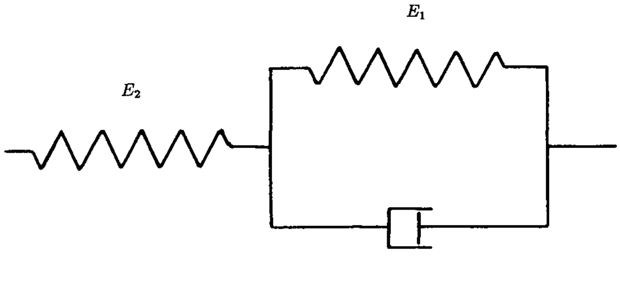

Fig. 2 Ideal three-element "limited" creep model.

Table 1 Differential elastic solution vs number of nodes for $P/P_e = 0.75$ and $a/l = 0.05$

Transverse deflection (cm) for various numbers of elements

$s = \hat{s}/l$	Number of elements 40	20	% diff[a]
0.0	0.000000	0.000000	—
0.1	0.062669	0.062751	0.13
0.2	0.249400	0.249700	0.12
0.3	0.556448	0.557103	0.12
0.4	0.977725	0.978855	0.12
0.5	1.504980	1.506695	0.11
0.6	2.128050	2.130438	0.11
0.7	2.835125	2.838262	0.11
0.8	3.613038	3.616978	0.11
0.9	4.447532	4.452313	0.11
1.0	5.323528	5.329169	0.11
$s = \hat{s}/l$	40	10	% diff
0.0	0.000000	0.000000	—
0.1	0.062669	0.063015	0.55
0.2	0.249400	0.250858	0.59
0.3	0.556448	0.559534	0.56
0.4	0.977725	0.983259	0.57
0.5	1.504980	1.513218	0.55
0.6	2.128050	2.139785	0.55
0.7	2.835125	2.850330	0.54
0.8	3.613038	3.632429	0.54
0.9	4.447532	4.470819	0.52
1.0	5.323528	5.351315	0.52

[a]% differences are with respect to 40-element solution.

Table 2 Integral elastic solution vs number of nodes for $P/P_e = 0.75$ and $a/l = 0.05$

Transverse deflection (cm) for various numbers of elements

$s = \hat{s}/l$	Number of elements 40	20	% diff[a]
0.0	0.000000	0.000000	—
0.1	0.062525	0.062616	0.15
0.2	0.248836	0.249238	0.16
0.3	0.555208	0.555981	0.14
0.4	0.975561	0.977115	0.16
0.5	1.501648	1.503906	01.5
0.6	2.123316	2.126658	0.16
0.7	2.828762	2.833050	0.15
0.8	3.604837	3.610412	0.16
0.9	4.437309	4.443969	0.15
1.0	5.311148	5.319194	0.15
$s = \hat{s}/l$	40	10	% diff
0.0	0.000000	0.000000	—
0.1	0.062525	0.062944	0.67
0.2	0.248836	0.250833	0.80
0.3	0.555208	0.559112	0.70
0.4	0.975561	0.981829	0.64
0.5	1.501648	1.512425	0.72
0.6	2.123316	2.137987	0.69
0.7	2.828762	2.847177	0.65
0.8	3.604837	3.629746	0.69
0.9	4.437309	4.466392	0.66
1.0	5.311148	5.348440	0.70

[a]% differences are with respect to 40-element solution.

Table 3 Comparison[a] of integral and differential[b] elastic solutions for various loads with $a/l = 0.05$

$s = \hat{s}/l$	Integral	Differential	% diff[c]	Angle, deg
		$P/P_e = 0.25$		
0.0	0.000000	0.000000	—	0.00
0.1	0.006642	0.006645	0.04	0.25
0.2	0.026543	0.026538	−0.02	0.50
0.3	0.059548	0.059550	0.00	0.74
0.4	0.105461	0.105489	0.03	0.98
0.5	0.164059	0.164056	0.00	1.22
0.6	0.234887	0.234907	0.01	1.44
0.7	0.317525	0.317579	0.02	1.66
0.8	0.411579	0.411592	0.00	1.87
0.9	0.516270	0.516329	0.01	2.07
1.0	0.631223	0.631182	−0.01	2.25
		$P/P_e = 0.50$		
0.0	0.000000	0.000000	—	0.00
0.1	0.021039	0.021044	0.02	0.79
0.2	0.083962	0.083932	−0.04	1.57
0.3	0.187808	0.187828	0.01	2.33
0.4	0.331320	0.331511	0.06	3.07
0.5	0.513103	0.513077	0.00	3.76
0.6	0.730283	0.730400	0.02	4.40
0.7	0.980300	0.980618	0.03	5.01
0.8	1.260747	1.260810	0.01	5.52
0.9	1.566974	1.567304	0.02	6.01
1.0	1.896801	1.896542	−0.01	6.38
		$P/P_e = 0.75$		
0.0	0.000000	0.000000	—	0.00
0.1	0.062944	0.063015	0.11	2.37
0.2	0.250833	0.250858	0.01	4.68
0.3	0.559112	0.559534	0.08	6.91
0.4	0.981829	0.983259	0.15	9.03
0.5	1.512425	1.513218	0.05	10.97
0.6	2.137987	2.139785	0.08	12.68
0.7	2.847177	2.850330	0.11	14.23
0.8	3.629746	3.632429	0.07	15.41
0.9	4.466392	4.470819	0.10	16.44
1.0	5.348440	5.351315	0.05	17.04

Transverse deflection (cm) from various solutions.

[a]Comparisons based on results from 10-element models. [b]Differential solution employing an exact sinϕ formula. [c]% differences are with respect to integral solution.

Table 4 Comparison[a] of integral and differential[b] elastic solutions for various loads with $a/l = 0.5$

$s = \hat{s}/l$	Integral	Differential	% diff[c]	Angle, deg
		$P/P_e = 0.25$		
0.0	0.000000	0.000000	—	0.00
0.1	0.006642	0.006645	0.00	0.25
0.2	0.026543	0.026538	−0.02	0.50
0.3	0.059548	0.059550	0.00	0.74
0.4	0.105461	0.105489	0.03	0.98
0.5	0.164059	0.164056	0.00	1.22
0.6	0.234887	0.234907	0.01	1.44
0.7	0.317525	0.317579	0.02	1.66
0.8	0.411579	0.411592	0.00	1.87
0.9	0.516270	0.516329	0.01	2.07
1.0	0.631223	0.631182	−0.01	2.25
		$P/P_e = 0.50$		
0.0	0.000000	0.000000	—	0.00
0.1	0.021039	0.021046	0.04	0.79
0.2	0.083962	0.083932	−0.04	1.57
0.3	0.187808	0.187830	0.01	2.33
0.4	0.331320	0.331511	0.06	3.07
0.5	0.513103	0.513080	0.00	3.76
0.6	0.730283	0.730402	0.02	4.40
0.7	0.980300	0.098620	0.03	5.01
0.8	1.260747	1.260813	0.01	5.52
0.9	1.566974	1.567307	0.02	6.01
1.0	1.896801	1.896547	−0.01	6.38
		$P/P_e = 0.75$		
0.0	0.000000	0.000000	—	0.00
0.1	0.062944	0.063017	0.12	2.37
0.2	0.250833	0.250868	0.01	4.68
0.3	0.559112	0.559559	0.08	6.91
0.4	0.981829	0.983305	0.15	9.03
0.5	1.512425	1.513286	0.06	10.97
0.6	2.137987	2.139881	0.09	12.68
0.7	2.847177	2.850459	0.12	14.23
0.8	3.629746	3.632594	0.08	15.41
0.9	4.466392	4.471020	0.10	16.44
1.0	5.348440	5.351554	0.06	17.04

Transverse deflection (cm) from various solutions.

[a]Comparisons based on results from 10-element models. [b]Differential solution employing an approximate sinϕ formula. [c]% differences are with respect to integral solution.

tensionality" of the integral model. These changes did produce a differential model with an effectively inextensional centroidal axis. It was anticipated that this would further improve the correlation between the differential and integral results. Unfortunately, such was not the case.

When the angle of rotation is very small, such as one that results from a low level of loading and minimal eccentricity, all formulations provide virtually identical predictions. Increases in the angle of rotation, however, due to increases in loading or eccentricity or both, cause the modified differential predictions to diverge from those of the others. This divergence between results increased with both load magnitude and eccentricity.

This behavior is attributed to the manner in which the modified numerical model handles the end deflection of the beam-column. In the modified model, the end of the beam-column effectively moves only in the vertical direction (see Fig. 1). The standard differential model as well as the integral model, however, include influences generated when the end can move both vertically and horizontally. Thus, for any given vertical deflection, the horizontal movement that occurs in the integral and unmodified differential models acts to increase the angle of rotation. This, in turn, reduces the magnitude of the applied moment [see Eq. (23)]. Therefore, at any particular given vertical deflection, the moment loading in the standard formulation model is lower than that in the modified version. Effectively, the moment decreases a greater amount in the unmodified model than it does in the modified model at equivalent amounts of transverse deflection. This, in turn, implies that the beam-column of the unmodified model would not deflect as much as the one of the modified model would.

The implication is that the numerical modeling of the influence of deformation on loading is an important factor. This conclusion is consistent with the observations made concerning how the structure of the integral equation, Eq. (5), changes as a result of the interaction between loading and deflection. Additionally, it should be noted that neglecting centroidal axis strain in the differential technique does not necessarily provide an effect equivalent to the assumption of inextensionality in the integral techniques. This is attributed to the fact that the elimination of the centroidal axis strain in the differential formulation can be accomplished only at the expense of reducing the actual coupling between deformation and loading.

For both methods, the initial elastic deflection of the beam-column provides the initial condition for the viscoelastic deformation. Consequently, any differences in the initial elastic responses predicted by the two methods will only be accentuated during the subsequent period of time-dependent behavior. The comparisons discussed demonstrate that the two methods provide virtually identical predictions of initial elastic deformation. Table 6 provides a typical comparison for the integral and the differential (exact sinϕ) method predictions for the viscoelastic deflection of the beam-column over a period of two

Table 5 Comparison[a] of integral and modified differential[b] elastic solutions for various loads with $a/l = 0.05$

$s = \hat{s}/l$	Integral	Differential	% diff[c]	Angle, deg
		$P/P_e = 0.25$		
0.0	0.000000	0.000000	—	0.00
0.1	0.006642	0.006645	0.00	0.25
0.2	0.026543	0.026533	−0.04	0.50
0.3	0.059548	0.059548	0.00	0.74
0.4	0.105461	0.105479	0.02	0.98
0.5	0.164059	0.164048	−0.01	1.22
0.6	0.234887	0.234894	0.00	1.44
0.7	0.317525	0.317576	0.02	1.66
0.8	0.411579	0.411589	0.00	1.87
0.9	0.516270	0.516349	0.02	2.07
1.0	0.631223	0.631210	0.00	2.25
		$P/P_e = 0.50$		
0.0	0.000000	0.000000	—	0.00
0.1	0.021039	0.021067	0.13	0.79
0.2	0.083962	0.084005	0.05	1.57
0.3	0.187808	0.188041	0.12	2.33
0.4	0.331320	0.331889	0.17	3.07
0.5	0.513103	0.513776	0.13	3.76
0.6	0.730283	0.731457	0.16	4.40
0.7	0.980300	0.982246	0.20	5.01
0.8	1.260747	1.263051	0.18	5.52
0.9	1.566974	1.570406	0.22	6.01
1.0	1.896801	1.900517	0.20	6.38
		$P/P_e = 0.75$		
0.0	0.000000	0.000000	—	0.00
0.1	0.062944	0.064879	3.07	2.37
0.2	0.250833	0.258313	2.98	4.68
0.3	0.559112	0.576725	3.15	6.91
0.4	0.981829	0.014219	3.30	9.03
0.5	1.512425	1.562702	3.32	10.97
0.6	2.137987	2.212025	3.46	12.68
0.7	2.847177	2.950167	3.62	14.23
0.8	3.629746	3.763475	3.68	15.41
0.9	4.466392	4.636892	3.82	16.44
1.0	5.348440	5.554259	3.85	17.04

Transverse deflection (cm) from various solution

[a]Comparisons based on results from 10-element models. [b]Influences of centroidal axis strain terms suppressed. [c]% differences are with respect to integral solution.

Table 6 Comparison[a] of integral and differential[b] viscoelastic solutions to two time constants; $P/P_e = 0.50$ and $a/l = 0.05$

$s = \hat{s}/l$	Integral	Differential	% diff[c]	Angle, deg
		at time = 0		
0.0	0.000000	0.000000	—	0.00
0.1	0.021039	0.021044	0.02	0.79
0.2	0.083962	0.083932	−0.04	1.57
0.3	0.187808	0.187828	0.01	2.33
0.4	0.331320	0.331511	0.06	3.07
0.5	0.513103	0.513077	0.02	3.76
0.6	0.730283	0.730400	0.02	4.40
0.7	0.980300	0.980618	0.03	5.01
0.8	1.260747	1.260810	0.01	5.52
0.9	1.566974	1.567304	0.02	6.01
1.0	1.896801	1.896542	−0.01	6.38
		at time = τ_0		
0.0	0.000000	0.000000	—	0.00
0.1	0.038311	0.038326	0.04	1.44
0.2	0.152784	0.152725	−0.04	2.86
0.3	0.341170	0.341234	0.02	4.22
0.4	0.600532	0.600994	0.08	5.54
0.5	0.927608	0.927590	0.00	6.76
0.6	1.315809	1.316129	0.02	7.86
0.7	1.759290	1.760083	0.05	8.87
0.8	2.252647	2.252896	0.01	9.70
0.9	2.785532	2.786395	0.03	10.44
1.0	3.353191	3.352810	−0.01	10.95
		at time = $2\tau_0$		
0.0	0.000000	0.000000	—	0.00
0.1	0.048583	0.048611	0.06	1.83
0.2	0.193685	0.193629	−0.03	3.62
0.3	0.432178	0.432313	0.03	5.34
0.4	0.759968	0.760689	0.09	7.00
0.5	1.172517	1.172627	0.01	8.52
0.6	1.660764	1.661396	0.04	9.88
0.7	2.216699	2.218045	0.06	11.13
0.8	2.832971	2.833680	0.03	12.12
0.9	3.495617	3.497252	0.05	12.99
1.0	4.198267	4.198371	0.00	13.55

Transverse deflection (cm) for various solutions

[a]Comparisons based on results from 10-element models. [b]Differential solution employing an exact $\sin\phi$ formula. [c]% differences are with respect to integral solution.

material time constants. The viscoelastic model employed for these computations is the three-parameter "limited" creep material illustrated in Fig. 2. As noted previously, the material parameters were selected so that the material time constant τ_0 equals unity. The load and eccentricity ratios for this particular set of results were $P/P_e = 0.50$ and $a/l = 0.05$, respectively.

As demonstrated by this data, the high correlation between the integral and differential method predictions for the initial elastic deflections carries over directly to the viscoelastic analysis. The time-dependent deflection predicted by one technique is virtually indistinguishable from that predicted by the other. This indicates that the differential formulation methodology employed to account for the influence of viscoelastic strain provides the equivalent effect as the hereditary integral component of the integral formulation. As such, this lends high confidence to the differential solution methodology.

It should be noted that these particular numerical results are typical of other results obtained for higher, as well as lower, loads and eccentricities. Generally, the correlation between the solutions was not influenced by the magnitude of the loading or the amount of load eccentricity.

A minor, high-order-type influence was, however, noted. As the angle of rotation became very large, on the order of 45 deg, a small but distinct divergence in predicted deflections was observed. Typically, the rate of increase in deflection predicted by the differential formulation would begin to slightly exceed that predicted by the integral method. Normally, this could be observed as time approached two material time constant for the highest loads (P/P_e approaching unity) and with extremely large eccentricities. Under some conditions, it also could be observed as time exceeded four to five material time constants.

These observed differences between the two sets of predictions were still very small. Generally, they were on the order of 0.10%. Thus, from a practical viewpoint, they are totally negligible with respect to normal accuracy requirements for engineering computation. It is mentioned here only to indicate that, under conditions such as these, the accumulation of numerical errors may begin to influence the results. A comparison between the integral and the approximate $\sin\phi$ differential solution results was not included because the differences between the exact and approximate differential solution results are again so small as to be negligible.

The final item meriting discussion is the length of the time increment used in each of the formulations. Unlike the prior results, some differences do exist between the maximum allowable time-step increments for the integral and differential formulations. Additionally, the allowable time-step increment for the integral formulation exhibits a higher dependence on the actual angle of rotation than does the differential formulation.

In general, a relatively small time step increment must be used with the integral solution methodology. For example, the results previously presented typically employed a 0.01-time-step increment. As the length of this time step is increased, the accuracy of the solution decreases and tends to underpredict the deflection. This convergence "from below" is not surprising since the convolution integral is approximated as the sum of a finite number of terms.

In contrast, much larger time-step increments were used with the differential formulation. This is principally attributed to the high accuracy provided by the Runge-Kutta integration routine. Most of the results provided were developed using a 0.10 time step. The use of even larger time steps was also examined. It was found that time increments four to five times greater than 0.10 could be employed without significant changes in the calculated results. Additionally, the allowable length of this time-step increment tended to be rather insensitive to the angle of rotation. The allowable time step for the integral formulation, on the other hand, exhibited a high level of sensitivity to the angle of rotation. Larger angles of rotation required significantly shorter time steps for accurate results to be obtained.

These factors combine in a rather interesting manner with regard to which method of analysis is computationally more efficient. Typically, for the analysis of short periods of viscoelastic deformation, the integral solution method was two to three times faster than the differential method. This is attributed to two factors. The first is the comparitively slow Runge-Kutta integration procedure used in the differential formulation. For a short period of viscoelastic deformation, the calculation of the convolution integral of the integral formulation, requiring simple summation of a limited number of terms, can be performed much more rapidly.

The second factor is that the fixed-point iteration scheme of the integral formulation, although requiring more iterations than the Newton method, is also performed more rapidly since it is simply an algebraic operation. The Newton method, in contrast, requires inversion of the matrix, premultiplying the vector of trial function corrections, and then numerical evaluation through solution of the system of equations. Even for just a 10-element beam, this process is slow in comparison to the fixed-point iteration.

However, as the length of the period of viscoelastic deformation increases, this relative speed relationship reverses. Eventually, the differential formulation begins to generate solutions more rapidly than the integral method. In the example problem previously described, this generally occurred approximately between the second and third time constants. The reason for this change is directly related to the computation of the convolution integral of the integral technique. As time increases, the number of terms in the summation increases linearly. This, in turn, increases the number of algebraic operations that must be performed and therefore linearly increases the time need for each complete computation. In contrast, the speed of the Runge-Kutta integration routine is virtually independent of time. Thus, the continually increasing computational effort required in the integral technique eventually exceeds that need for the differential technique. This reverses the relative speed relationship.

Conclusions

Based on the results reported herein and elsewhere,[12] it is concluded that the differential formulation procedure presented can be employed for the analysis of quasistatic nonlinear one-dimensional viscoelastic problems. This conclusion is based directly on the high level of correlation between results developed using this formulation technique to those obtained with the previously published integral method for solution of such problems. Additionally, it is observed that both of these methods exhibit exceptionally similar accuracy characteristics with regard to the number of elements employed in the approximation. For both, a relatively low number of elements can be used without engendering any significant errors.

Acknowledgments

The research described has been performed under NASA Grant 3-534. The financial support provided by NASA is gratefully acknowledged by the authors. The authors also wish to extend their thanks and appreciation to Dr. C. C. Chamis of the NASA Lewis Research Center for his support and for the insights into the problem which he provided during our many technical discussions.

References

[1]Christensen, R. M., *Theory of Viscoelasticity, An Introduction*, Academic, New York, 1982.

[2]Rabotnov, Y. N., *Elements of Hereditary Solid Mechanics*, Mir Publications, Moscow, USSR, 1980.

[3]Schapery, R. A., "Approximate Methods of Transform Inversion for Viscoelastic Stress Analysis," *Proceedings of the 4th US National Congress on Applied Mechanics*, Vol. 2, 1962, pp. 1075–1085.

[4]Kraus, H., *Creep Analysis*, Wiley, New York, 1980.

[5]Libove, C., "Creep Buckling of Columns," *Journal of the Aeronautical Sciences*, Vol. 19, July, 1952, pp. 459–467.

[6]Zyczkowski, M., "Geometrically Non-Linear Buckling of Bars," *IUTAM Colloquium on Creep in Structures*, Academic, New York, 1962, pp. 307–325.

[7]Patel, S. A., "Buckling of Columns in the Presence of Creep," *The Aeronautical Quarterly*, Vol. 7, No. 2, April–June 1956, pp. 25–134.

[8]Hoff, N. J., "A Survey of the Theories of Creep Buckling," *Proceedings of the 3rd U.S. National Congress of Applied Mechanics*, 1958, pp. 29–49.

[9]Rogers, T. G. and Lee, E. H., "On the Finite Deflection of a Viscoelastic Cantilever," *Proceedings of the 4th U.S. National Congress on Applied Mechanics*, Vol. 2, 1962, pp. 977–987.

[10]Stubstad, J. M. and Simitses, G. J., "Bounding Solutions of Geometrically Nonlinear Viscoelastic Problems," *AIAA Journal*, Vol. 24, Dec. 1986, pp. 1843–1850.

[11]Thurston, G., "Newton's Method Applied to Problems in Nonlinear Mechanics," *Journal of Applied Mechanics*, Vol. 32, No. 2, 1965, pp. 383–388.

[12]Stubstad, J. M., "Nonlinear Thermoviscoelastic Analysis of Metallic Plane Curved Beams," Ph.D. Thesis, Georgia Inst. of Technology, Atlanta, GA, 1986.

[13]Vinogradov, A. M. "Nonlinear Effects in Creep Buckling Analysis of Columns," *Journal of Engineering Mechanics*, Vol. 111, No. 6, 1985, pp. 757–767.

[14]Vinogradov, A. M. and Wijewerra, H., "Theoretical and Experimental Studies on Creep Buckling," *Proceedings of the AIAA/ASME/ASCE/AHS 26th Structures, Structural Dynamics and Materials Conference*, AIAA, New York, 1985, Vol. 1, pp. 160–164.

[15]Tricomi, F. G., *Integral Equations*, Dover, New York, 1985, pp. 42–47.